Pair-correlation function in two-dimensional lattice gases

E. Scalas and R. Ferrando
Dipartimento di Fisica dell'Università di Genova, via Dodecaneso 33, 16146 Genova, Italy
(Received 2 June 1993)

The pair-correlation function in two-dimensional lattice gases is computed by means of three discretized classical equations for the structure of liquids: the hypernetted-chain, the Percus-Yevick, and the crossover integral equations. The equations are numerically solved by an iteration procedure. Two different systems are considered: the Ising-Peierls lattice gas with nearest-neighbor interactions and a model for O adsorbed on the W(110) surface, in which interactions up to the fourth neighbors are taken into account. The values of the pair-correlation function for nearest, next-nearest, and next-next-nearest neighbors are compared with the results of Monte Carlo simulations at four different coverages Θ ($\Theta=\frac{1}{8},\frac{1}{4},\frac{1}{2},\frac{3}{4}$) as functions of the lateral coupling. It turns out that the crossover integral equation gives the best agreement with Monte Carlo data in both systems, being accurate especially at low Θ, whereas the Percus-Yevick equation fails in a wide range of parameters.

PACS number(s): 61.20.Ne, 05.50.+q, 82.65.Dp, 82.65.My

I. INTRODUCTION

Two-dimensional lattice gases are the most widely employed models for the description of adsorbed monolayers on crystal surfaces [1–3]. In these systems the interactions between the adsorbed particles can be either short- or long-ranged. For example, for H-W(100) [3,4] a simple Ising model with only nearest-neighbor interactions is sufficient to reproduce the intensity of the low-energy electron-diffraction (LEED) spot of the $c(2\times2)$ structure at a coverage $\Theta=0.5$; for H-Pd(100) also second-neighbor interactions are necessary [5,6]; for O-W(110) interactions up to the fourth neighbors are important [7,8]; and, finally, for Na-W(110) dipolar interactions of infinite range must be taken into account [9]. Moreover, in many systems, three-body interactions are needed in order to explain the asymmetry of the phase diagram with respect to $\Theta=0.5$ [1,3].

The knowledge of the two-particle correlation function is important for the calculation of thermodynamic quantities: for example, the static structure factor $S(\mathbf{q})$ [10] (which, for adsorbed monolayers, is measured, for instance, by LEED [1]) at wave vector $\mathbf{q}=\mathbf{0}$ gives directly the compressibility equation for the system. Moreover, the knowledge of the pair-correlation function $g(\boldsymbol{l})$ is needed for the determination of dynamical properties such as the single-particle (or tracer) [11] and the collective (or chemical) diffusion coefficients [12].

In general, the calculation of the two-particle correlation function $g(\boldsymbol{l})$, where $\boldsymbol{l}$ is a lattice vector, is a rather difficult problem. In fact, few exact analytical results are known, essentially in the case of nearest-neighbor interactions at $\Theta=0.5$ [13,14], corresponding to the Ising model without magnetic field. It is known that in two dimensions the mean-field approximation [15] is rather poor. Moreover, when long-range interactions are present, many approximation techniques, such as the transfer matrix, and even the Monte Carlo simulations become rather cumbersome.

In this paper we adapt to lattice gases three well-known integral equations for the structure of liquids: the Percus-Yevick (PY), the hypernetted-chain (HNC) [10,16,17], and the crossover integral (CI) equations [18,19]. In a previous work [11] $g(\boldsymbol{l})$ was computed by solving the discretized form of another classical equation for the structure of liquids: the mean spherical approximation (MSA), in the case of nearest-neighbor interactions. It turns out that the MSA is accurate only at rather small lateral interactions, i.e., $|\beta J|<0.8$, where $\beta=1/k_BT$ and J is the nearest-neighbor coupling; at higher $|\beta J|$ the MSA seriously underestimates $g(\boldsymbol{l})$, especially in the attractive case ($J<0$).

The properties of the discretized forms of PY, HNC, and CI equations have been studied in the critical region in order to determine the critical point and the critical exponents [19–21]. The critical behavior of the Ising model is not correctly described by these equations either in two or in three dimensions. However, far away from the critical region, these equations should give a correct description of the structure of the lattice gas, as the MSA does. Here we solve the three equations and we calculate $g(\boldsymbol{l})$ for two different models: the first model is the Ising-Peierls lattice gas, where only repulsive or attractive nearest-neighbor interactions are present; in the second case we consider the system O-W(110), for which interactions up to the fourth-nearest neighbors must be considered. In both cases, we investigate the high-temperature region of the phase diagram, where a single disordered phase exists; the accuracy of the three equations is tested against Monte Carlo data and, where possible, against exact analytical results. Our aim is to check whether these equations can be safely used in order to compute the static correlations for different kinds of interactions between the particles, corresponding to different systems of interest in surface physics.

The paper is organized as follows. In Sec. II we sketch the numerical procedure; in Sec. III we present the results for the Ising-Peierls model on a square lattice; in

Sec. IV we consider a model for oxygen adsorbed on W(110). Finally, in Sec. V we present the conclusions and outline the direction for future work.

II. THEORY AND NUMERICAL PROCEDURE

Let us consider a two-dimensional (2D) lattice partially filled by identical particles. The lattice sites are denoted by the vectors $\boldsymbol{l}$. If only pairwise interactions between the particles are taken into account, the Hamiltonian of the lattice gas becomes of the following form:

$$H(\mathbf{n})=\tfrac{1}{2}\sum_{l,\mathbf{s}} V_{l-\mathbf{s}} n_l n_{\mathbf{s}} - \mu \sum_l n_l \ , \tag{2.1}$$

where a lattice configuration is denoted by $\mathbf{n}=\{n_l\}$ and each site occupation number n_l can assume only the values 0 and 1 (this accounts for the hard-sphere repulsion between the particles). $V_{l-\mathbf{s}}$ is the pairwise interaction and μ is the chemical potential which determines the coverage $\langle n_l \rangle = \Theta$.

The pair correlation function $g(\boldsymbol{l})$ is defined as

$$g(\boldsymbol{l})=\frac{\langle n_{\mathbf{0}} n_l \rangle}{\Theta^2} \quad \text{for } \boldsymbol{l}\neq\mathbf{0} \ , \tag{2.2}$$

$$g(\mathbf{0})=0 \ . \tag{2.3}$$

The quantity $\Theta g(\boldsymbol{l})$ is the probability of site $\boldsymbol{l}$ being occupied if site $\mathbf{0}$ is full; therefore the maximum value that $g(\boldsymbol{l})$ can attain at a fixed coverage Θ is simply Θ^{-1} (in this case also site $\boldsymbol{l}$ is occupied with probability 1).

The pair-correlation function is calculated by adapting the classical integral equations for the structure of fluids to the lattice gas. As specified in the Introduction, we consider three different equations which have been widely employed in the computations of the structure of simple fluids [10,16]: the PY, HNC, and CI equations.

Let us introduce the direct correlation function $c(\boldsymbol{l})$, which is connected to $g(\boldsymbol{l})$ by the Ornstein-Zernike relation [10]:

$$h(\boldsymbol{l})=c(\boldsymbol{l})+\Theta\sum_{\mathbf{s}} c(\boldsymbol{l}-\mathbf{s})h(\mathbf{s}) \ , \tag{2.4}$$

where

$$h(\boldsymbol{l})=g(\boldsymbol{l})-1 \ . \tag{2.5}$$

The three equations are defined by different closure relations. For $\boldsymbol{l}=\mathbf{0}$ the closure relation is given by Eq. (2.3) for all of them. For $\boldsymbol{l}\neq\mathbf{0}$ the PY is defined by [10,17]

$$c(\boldsymbol{l})=[1-\exp(\beta V_l)][h(\boldsymbol{l})+1] \tag{2.6}$$

and the HNC equation by

$$c(\boldsymbol{l})=-\beta V_l + h(\boldsymbol{l}) - \ln[h(\boldsymbol{l})+1] \ . \tag{2.7}$$

Finally, the CI equation assumes that the closure relation is given by Eq. (2.7) only for the lattice sites $\boldsymbol{l}$ within the range of the potential, whereas $c(\boldsymbol{l})=0$ outside the range of the potential. For infinite-range potentials the HNC and CI equations coincide.

Let us briefly explain the hypothesis leading to the CI equation, which is perhaps the less known among the three. In the CI equation the bridge function $E(\boldsymbol{l})$ [10] is approximated as follows [19]. At short distances (i.e., within the range of the potential), $E(\boldsymbol{l})$ is assumed to coincide with the hard-sphere value of the bridge function. Noticing that the equivalent of hard spheres is the lattice gas without lateral interactions, for which the bridge function vanishes, it turns out that $E(\boldsymbol{l})=0$ within the range of the potential; this leads to the HNC closure at short distances. Outside the range of the potential the MSA is assumed to be a good approximation; for the MSA one has that $E(\boldsymbol{l})=\ln[g(\boldsymbol{l})]-h(\boldsymbol{l})$ and therefore $c(\boldsymbol{l})=0$.

The pair-correlation function $h(\boldsymbol{l})$ is computed by solving the three equations through an iteration procedure on a lattice of finite size. From (2.3) and (2.4) we find

$$c(\mathbf{0})=-\frac{1}{1-\Theta}\left[1+\Theta\sum_{\mathbf{s}\,(\neq\mathbf{0})} c(\mathbf{s})h(\mathbf{s})\right] \ ; \tag{2.8}$$

then the Ornstein-Zernike relation yields the following expression for $h(\boldsymbol{l})$ at $\boldsymbol{l}\neq\mathbf{0}$:

$$h(\boldsymbol{l})=\frac{1}{1-\Theta c(\mathbf{0})}\left[c(\boldsymbol{l})+\Theta\sum_{\mathbf{s}\,(\neq\boldsymbol{l})} c(\boldsymbol{l}-\mathbf{s})h(\mathbf{s})\right] \ . \tag{2.9}$$

Starting from a trial correlation function $h_1(\boldsymbol{l})$ we obtain $c_1(\boldsymbol{l})$ from the proper closure relation and from Eq. (2.8); then $c_1(\boldsymbol{l})$ and $h_1(\boldsymbol{l})$ are inserted in Eq. (2.9) in order to get the intermediate quantity $\tilde{h}(\boldsymbol{l})$. The new trial correlation function $h_2(\boldsymbol{l})$ is chosen to be

$$h_2(\boldsymbol{l})=\alpha\tilde{h}(\boldsymbol{l})+(1-\alpha)h_1(\boldsymbol{l}) \ , \tag{2.10}$$

where $0<\alpha\leq 1$ is chosen in order to achieve a faster convergence. Usually we set $\alpha=1$; however, in some cases (for example, for a potential with only nearest-neighbor repulsive interactions) convergence is faster with a smaller α. The procedure is repeated until

$$|h_{n+1}(\boldsymbol{l})-h_n(\boldsymbol{l})|<\epsilon \ ; \tag{2.11}$$

for every $\boldsymbol{l}$; ϵ is a small number, typically $\epsilon=10^{-6}$. The convergence is also checked by changing the size of the lattice; however, at the interaction strengths considered in the examples treated in the following sections, a 40×40 lattice is always sufficient.

III. NEAREST-NEIGHBOR INTERACTIONS

In this section we study the two-point correlation function $h(\boldsymbol{l})$ in the case of the Ising-Peierls lattice gas on a square lattice, i.e., throughout this section we set

$$V_{l-\mathbf{s}}=J \tag{3.1}$$

if the sites $\boldsymbol{l}$ and $\mathbf{s}$ are nearest neighbors and $V_{l-\mathbf{s}}=0$ otherwise. If $J>0$ the interactions are repulsive; if $J<0$ they are attractive. Besides, we consider values of $|\beta J|$ lower than the critical value 1.76.

In Figs. 1–4 we plot $h(\boldsymbol{l})$ for nearest (1,0), next-nearest (1,1), and next-next-nearest (2,0) neighbors, as a function of the interaction strength βJ for $\Theta=\frac{1}{8}, \frac{1}{4}, \frac{1}{2}$, and $\frac{3}{4}$. The

results of the PY equation are represented by the dashed lines, the dot-dashed lines give h in the HNC approximation whereas the solid lines are the values obtained by the CI equation.

The black dots represent the results of Monte Carlo simulations, which are used in order to test the validity of the various approximations. We work with a square lattice of $M=32\times32=1024$ sites and periodic boundary conditions. We are interested in the behavior of the lattice gas for low lateral coupling, far from the critical point; therefore we find a size 32×32 sufficient for our purposes. We compute the correlation function for both attractive and repulsive interactions below the critical point: $\beta J=\pm0.4$, ±0.8, ±1.2, ±1.5. The correlation function is given by

$$g(l)=\frac{1}{4\Theta^2M^2}\left\langle\sum_s n_s n_{s+l}\right\rangle , \tag{3.2}$$

where $\langle\ \rangle$ denotes the average over many independent Monte Carlo runs. After an appropriate thermalization we compute $g(1,0)$, $g(1,1)$, and $g(2,0)$ over 1000 independent realizations every five Monte Carlo steps per particle, until their values become independent of the Monte Carlo time.

At $\Theta=\frac{1}{8}$ (Fig. 1) the three approximations coincide for repulsive interactions and they give values of h in very good agreement with Monte Carlo simulations. As an example, for $\beta J=1.5$ the three results for $h(1,0)$ are accurate to 1%. In the case of attractive interactions the three approximations are no longer coincident. In particular, our program is unstable for the HNC equation if $\beta J<-1$. We discuss this point at the end of this section. It turns out that the CI equation is the better approximation to the Monte Carlo data. In the range $-1.5<\beta J<0$ the values of $h(1,0)$ predicted by the CI equation differ from the Monte Carlo results by less than 1%.

Things are not very different at $\Theta=\frac{1}{4}$ (Fig. 2), even if the CI result deviates slightly from the other two approximations in the repulsive case, where the PY and HNC equations give the best results. As an example, if $\beta J=1.5$ then the PY value for $h(2,0)$ is accurate to 4%, whereas the CI value is within 12% of the Monte Carlo point. However, when $h(1,0)$ is taken into account the CI relative error is only 3%. The CI approximation is again the best in the attractive region, its accuracy being always better than 7% for $h(1,0)$. Here the PY equation is good only in a limited coupling range ($-0.4<\beta J<0$) and it fails elsewhere and the HNC becomes soon unstable.

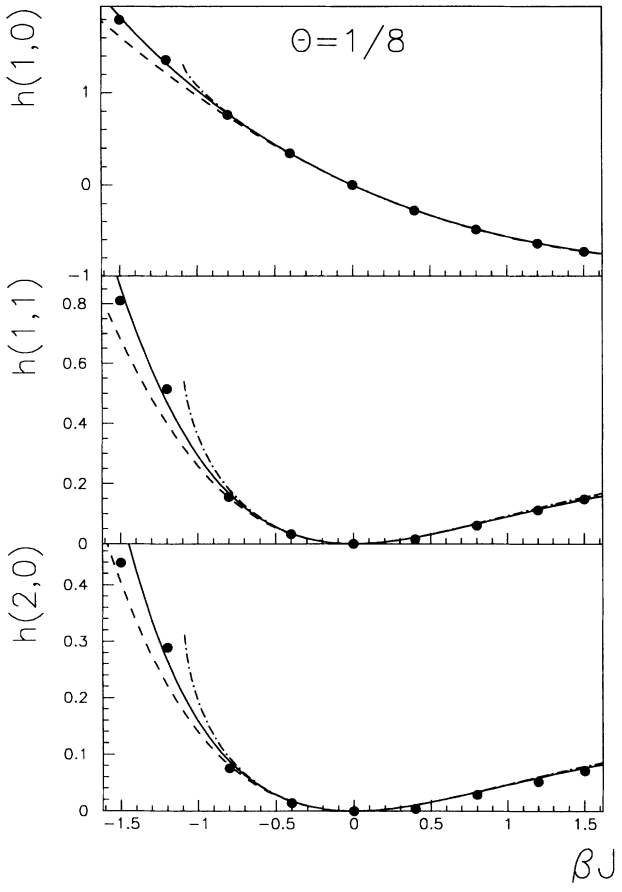

FIG. 1. Ising-Peierls lattice gas: pair-correlation function $h(l)$ for first (upper panel), second (intermediate panel), and third (lower panel) neighbors at $\Theta=\frac{1}{8}$ as functions of the lateral coupling. Solid lines: CI equation. Dashed lines: PY equation. Dot-dashed lines: HNC equation. The black dots are the result of the Monte Carlo simulations.

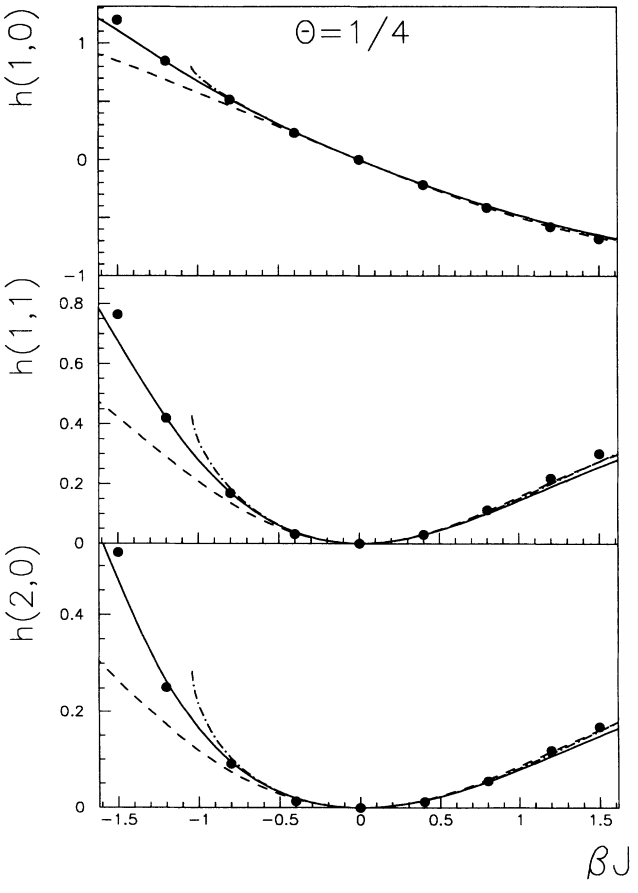

FIG. 2. The same as in Fig. 1, but at $\Theta=\frac{1}{4}$.

An exact result is available only in the case $\Theta=\frac{1}{2}$ (Fig. 3), where the lattice gas is equivalent to the Ising model with nearest-neighbor interactions and without a magnetic field. This equivalence can be easily shown using the transformation

$$n_l=\frac{1-\sigma_l}{2} . \tag{3.3}$$

Therefore $\sigma_l=-1$ corresponds to an occupied site and $\sigma_l=+1$ corresponds to an empty site. At $\Theta=\frac{1}{2}$ we have:

$$\langle n_0 n_l\rangle=\tfrac{1}{4}(\langle\sigma_0\sigma_l\rangle+1) . \tag{3.4}$$

Formula (5.4) of Cheng and Wu's paper [14] gives an integral representation of $\langle\sigma_0\sigma_l\rangle$. For $l=\mathbf{b}_1=(1,0)$, one obtains [13]:

$$\langle\sigma_0\sigma_{\mathbf{b}_1}\rangle=\coth(\beta J/2)[a(k)A(\beta J;k)-b(k)B(\beta J;k)] , \tag{3.5}$$

where

$$k=(\sinh\beta J/2)^{-2} , \tag{3.6}$$

$$A(\beta J;k)=\int_0^{\beta J/2}\frac{dx}{(1+k^2\sinh^2x)^{1/2}} , \tag{3.7}$$

$$B(\beta J;k)=\int_0^{\beta J/2}\frac{\tanh^2x}{(1+k^2\sinh^2x)^{1/2}}dx , \tag{3.8}$$

$$a(k)=\frac{2}{\pi}\mathcal{E}(k) , \tag{3.9}$$

$$b(k)=\frac{2}{\pi}(1-k)\mathcal{K}(k_1) , \tag{3.10}$$

where $\mathcal{K}$ and $\mathcal{E}$ are the complete elliptic integrals of the first and second kind, respectively, and $k_1=2k^{1/2}/(1+k)$. The results of the three approximations for $h(1,0)$ are compared with the exact result in Fig. 3 (upper panel). The PY approximation seems to work better in the repulsive region, but one has to stress that the overall trend of the PY curve does not reflect that of the exact curve. At this coverage the HNC and CI curves virtually coincide and they give rather good results if $|\beta J|<0.8$. In the attractive case the PY equation greatly underestimates the correlations if $\beta J<-0.4$. These considerations are true even for $h(1,1)$ and $h(2,0)$.

At $\Theta=\frac{3}{4}$ (Fig. 4), like at $\Theta=\frac{1}{2}$, the HNC and CI approximations are in good agreement with Monte Carlo data if $|\beta J|<0.8$ [the relative error being less than 9%

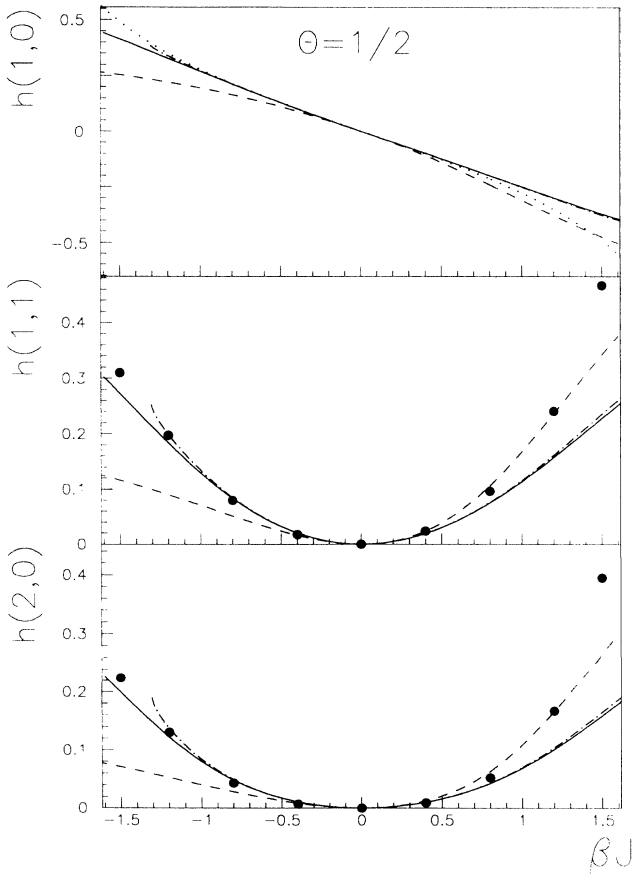

FIG. 3. The same as in Fig. 1, but at $\Theta=\frac{1}{2}$. In the upper panel the results of the three equations are compared with the exact solution represented by the dotted line (see text for explanation).

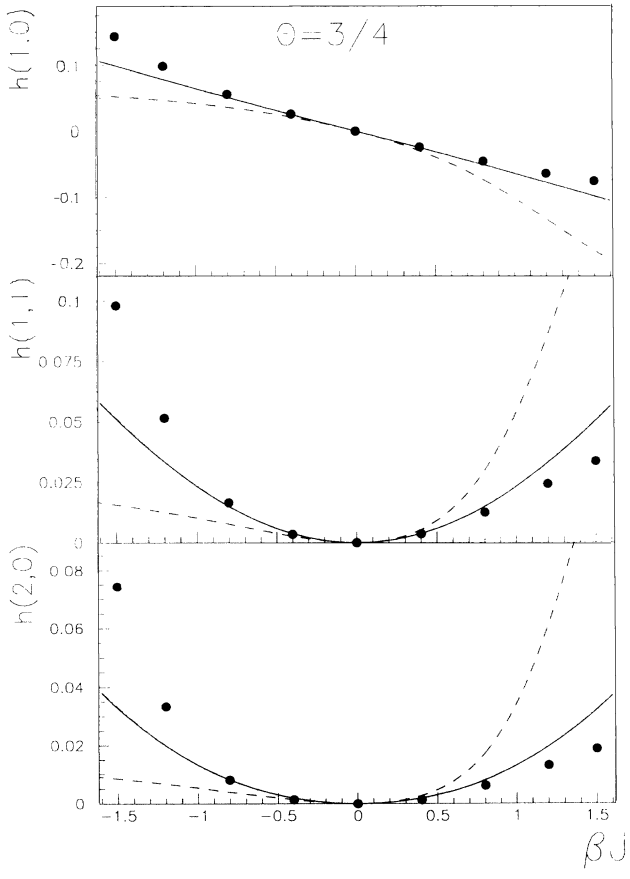

FIG. 4. The same as in Fig. 1, but at $\Theta=\frac{3}{4}$.

for $h(1,0)$]. On the contrary the PY equation completely fails.

More than once we have remarked that the CI and the HNC equations give almost the same results. This is true of nearest, next-nearest, and next-next-nearest neighbors. Of course, this is not necessarily the case in the asymptotic region.

Before closing this section we must remind the reader that the HNC equation gives unstable solutions in the explored attractive range. In Fig. 5 we report the "spinodal" curve separating the regions of stability from those of instability. Recently, for the case of three-dimensional liquids and for different interaction potentials, it has been shown that the line separating stable and unstable solutions is not a true spinodal line [22]. This might happen also in our case; however, we have not investigated this point in detail because it is outside the scope of the present work.

From the above discussion we can conclude that the CI equation gives the best results at low coverages ($\Theta \leq \frac{1}{4}$). It is almost exact in the attractive region, whereas it is only slightly worse than PY for repulsive interactions. Moreover it is not affected with the instabilities of the HNC equation. At higher coverages it gives reliable values in the range $-1.2 \leq \beta J \leq 0.8$ at $\Theta=\frac{1}{2}$ and in the range $-0.8 \leq \beta J \leq 0.8$ at $\Theta=\frac{3}{4}$.

IV. MODEL FOR O-W(110)

The system O-W(110) at submonolayer coverages has been experimentally studied both from the point of view of the determination of the phase diagram [7,23] and of the measure of the collective diffusion coefficient [12]. It has been shown that in this system lateral interactions up to fourth-nearest-neighbors are important [7]. In order to explain the asymmetry of the phase diagram with respect to $\Theta=\frac{1}{2}$, three-particle interactions have been introduced also [8]; however, their coupling constant is not large. In the following the three-body interactions will be neglected; this implies that at $\Theta>\frac{1}{2}$ the model here is no longer a good description of the system O-W(110). However, at low coverages, the three-body interactions should be really negligible. The unit cell of the lattice of adsorption sites is a rhombus (see Fig. 6); there are four first neighbors at a distance $\sqrt{3}a/2$ (one of them is indicated as $\mathbf{b}_1$ in the figure), two second neighbors ($\mathbf{b}_2$) at a, two third neighbors ($\mathbf{b}_3$) at $\sqrt{2}a$, and four fourth neighbors ($\mathbf{b}_4$) at $\sqrt{3}a$. The corresponding interaction energies are [7]

$$J_1=-2.1 \text{ kcal/mole} ,$$
$$J_2=J_3=1.7 \text{ kcal/mole} , \quad (4.1)$$
$$J_4=-0.7 \text{ kcal/mole} .$$

From these values of the lateral interactions it follows that second and third neighbors are equivalent for what concerns the equilibrium properties of the system; this implies that this model can be studied also by transforming the rhombus into a square [8], i.e., by considering the diagonals of the rhombus as if they were equal. Therefore in the following we will refer to $h(\mathbf{b}_2)$, remembering that $h(\mathbf{b}_3)=h(\mathbf{b}_2)$.

The results $h(\mathbf{b}_1)$, $h(\mathbf{b}_2)$, and $h(\mathbf{b}_4)$ according to the three approximations are shown, as functions of the inverse temperature, in Figs. 7–10. As in Sec. II we consider four different coverages and compare the theoretical results to those of a Monte Carlo simulation of the lattice gas. We consider temperatures at which only the disordered phase exists; the ordered phase is a $p(2\times1)$ which is stable below 720 K at $\Theta=\frac{1}{2}$ and below about 500 K at $\Theta=\frac{1}{4}$ (see the phase diagram in Ref. [23] or [12]).

At every coverage and temperature, $h(\mathbf{b}_1)$ and $h(\mathbf{b}_4)$ are positive whereas $h(\mathbf{b}_2)$ and $h(\mathbf{b}_3)$ are negative; this fact is not surprising since the first- and fourth-neighbor interactions are attractive and the other ones are repulsive. The overall effect of the interactions of Eq. (4.1) is to enhance the fourth-neighbor correlations. In fact at sufficiently low temperature the latter correlations become stronger than the nearest-neighbor ones. As the coverage increases, this happens at higher and higher temperatures: for instance, below 550 K at $\Theta=\frac{1}{8}$ and below 1000 K at $\Theta=\frac{1}{4}$.

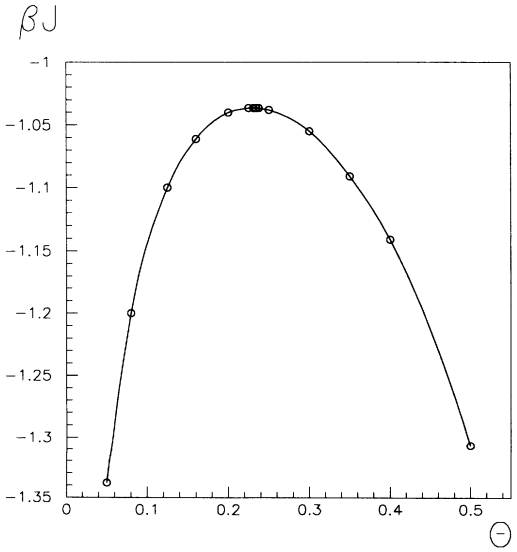

FIG. 5. The "spinodal" curve for the HNC equation. The open circles are calculated solving the HNC by the iteration procedure described in the text; the solid line is a guide for the eye.

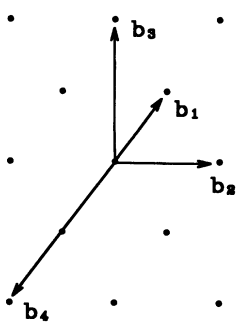

FIG. 6. The lattice of adsorption sites for O on W(110).

At low coverage ($\Theta=\frac{1}{8}$, Fig. 7) the behavior of the three correlations is very well reproduced by the CI equation, which is in very good quantitative agreement with the Monte Carlo data even well below 1000 K, i.e., in the temperature range of major interest from the experimental point of view: the differences are within 5% down to 600 K and within 8% down to 500 K. As for the HNC equation, it shows an instability at 627 K; this instability is analogous to that found for the model with nearest-neighbor attractive interactions. However, above 650 K the results of the HNC equation practically coincide with those of the CI equation and therefore they are in very good agreement with the Monte Carlo points. On the contrary, the PY equation is satisfactory only at very high temperatures, above 1100 K, even in this low-coverage case; below that temperature the results of the PY equation are in apparent disagreement with the Monte Carlo points. In particular, the PY equation predicts that the first and the fourth neighbors are less correlated than they should be, while the second and the third neighbors seem more correlated [notice that the strength of the correlation is given by the absolute value of $h(\boldsymbol{l})$].

At $\Theta=\frac{1}{4}$, the CI equation is still a satisfactory approximation at temperatures of experimental interest. This fact can be seen in Fig. 8, where a temperature range

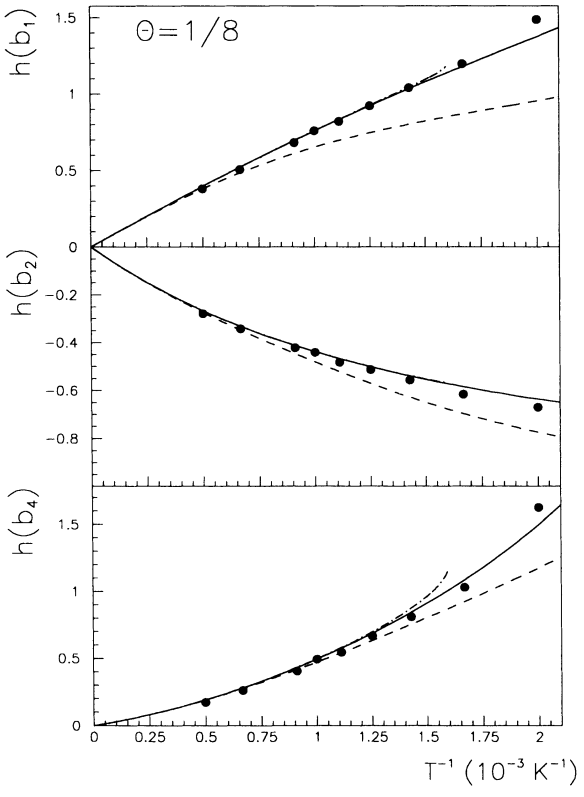

FIG. 7. O-W(110): pair-correlation function $h(\boldsymbol{l})$ for first (upper panel), second or third (intermediate panel), and fourth (lower panel) neighbors at $\Theta=\frac{1}{8}$ as functions of the inverse temperature. Solid lines: CI equation. Dashed lines: PY equation. Dot-dashed lines: HNC equation. The black dots are the result of the Monte Carlo simulations.

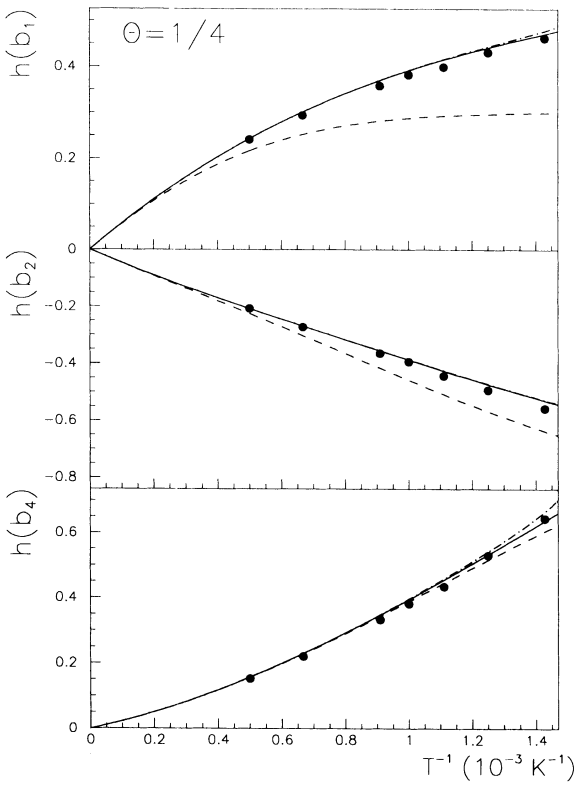

FIG. 8. The same as in Fig. 7, but at $\Theta=\frac{1}{4}$.

down to 700 K is reported. The maximum difference between the CI results and the Monte Carlo data is of about 2% for what concerns $h(\mathbf{b}_1)$ and $h(\mathbf{b}_4)$, whereas it is of 5% for what concerns $h(\mathbf{b}_2)$. In this temperature range the HNC gives essentially the same results as the CI (the instability is around 670 K); the PY equation well reproduces only the behavior of $h(\mathbf{b}_4)$, being unsatisfactory for the other correlations.

Also at $\Theta=\frac{1}{2}$ (Fig. 9), CI and HNC equations give almost coincident results down to 700 K. Both approximations are less precise than at lower coverage, being, however, in good agreement with the Monte Carlo data for a rather wide range of temperatures. For instance, $h(\mathbf{b}_1)$ is calculated with a precision better than 7% down to 900 K; below 800 K both the equations are not able to reproduce the correct nearest-neighbor correlations because the critical temperature (721 K) is approached. As the neighbor distance increases, the agreement between the equations and the Monte Carlo data improves: $h(\mathbf{b}_2)$ and $h(\mathbf{b}_4)$ are calculated with a precision better than 10% down to 800 and 750 K, respectively. As for the PY equation, it does not give satisfactory results at any temperature of physical interest.

At $\Theta=\frac{3}{4}$ (Fig. 10), CI and HNC equations are within 10% only down to about 1000 K for what concerns $h(\mathbf{b}_1)$ and $h(\mathbf{b}_3)$; better results are obtained for $h(\mathbf{b}_4)$. Also in this case the PY equation gives the worst results. We remark, however, that, at such a high coverage, the two-body interactions specified by Eq. (4.1) are not sufficient

to correctly describe O-W(110); three-body interactions are no longer negligible.

Finally, we remark that the CI equation describes accurately the pair correlations for this model in a wide range of temperatures at coverages $\Theta \leq \frac{1}{2}$; at higher Θ the CI approximation is accurate only at very high temperatures. At temperatures below 700 K and at low coverages, the validity of the HNC equation is limited by its instability. Where the HNC is stable, it gives essentially the same results as the CI. Of course, the results are the same at least for correlations up to the fourth neighbors. The asymptotic behavior for large distances is different; according to the HNC, long-distance correlations are stronger than according to the CI. The PY equation is not satisfactory even at low coverages and it cannot be employed to describe O-W(110) in any parameter range of physical interest.

V. CONCLUSIONS

We started the present study in order to find efficient methods to compute the static correlations in two-dimensional lattice gases, which are the most widely employed models for the description of adsorbed layers on crystal surfaces. We are interested in finding a general method which can be used both in systems with short-range and with long-range interactions. In adsorbed layers many examples of systems with very different lateral interactions can be found [3].

The pair-correlation function is important because it allows one to compute static properties of experimental interest [1,12] such as the static structure factor and the compressibility [10]; moreover, it is used in the calculation of dynamical quantities such as the coherent and incoherent dynamic structure factors and the chemical and tracer diffusion coefficients [11,24].

In this paper we have shown that the discretized classical equations for the structure of liquids can give a rather accurate description of the pair correlations in two-dimensional lattice gases. In particular, the crossover integral equation can be satisfactorily applied in a large range of temperatures and coverages. In fact, we have shown that the CI equation works well both in the case of nearest-neighbor interactions and in the case of O-W(110). As far as repulsive interactions are present, the HNC equation gives practically the same short-range correlations as the CI, at least in the interaction range considered here. When the interactions present an attractive part, the discretized HNC shows instabilities, which, at low coverages, are well above criticality. As for the PY equation, we obtain satisfactory results only in the case of repulsive nearest-neighbor interactions at rather low coverages. From the above discussion, we can conclude that the CI equation gives the best results.

However, there are still some regions of parameters, in particular the high-coverage region, which are not described accurately by any of the equations considered here. Besides, all three equations fail to describe the critical behavior of lattice gases. Therefore different approaches should be used; good candidates could be the PY2 and HNC2 equations [10] and the hierarchical refer-

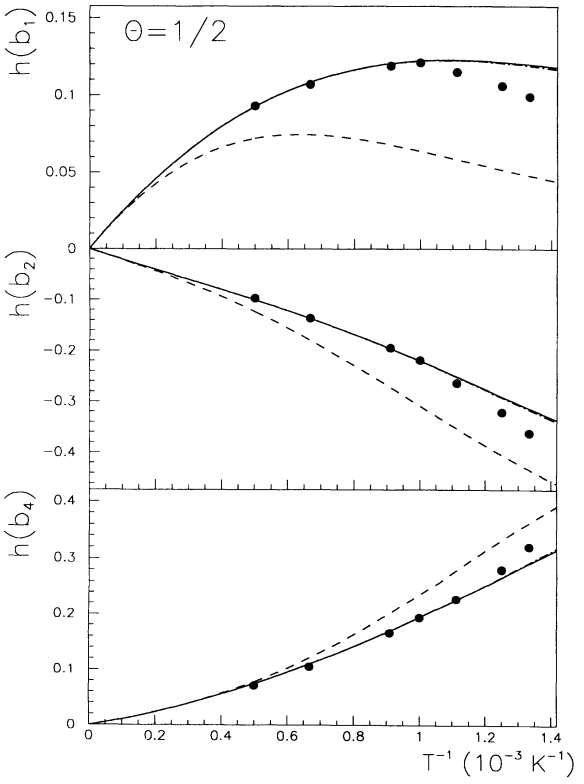

FIG. 9. The same as in Fig. 7, but at $\Theta = \frac{1}{2}$.

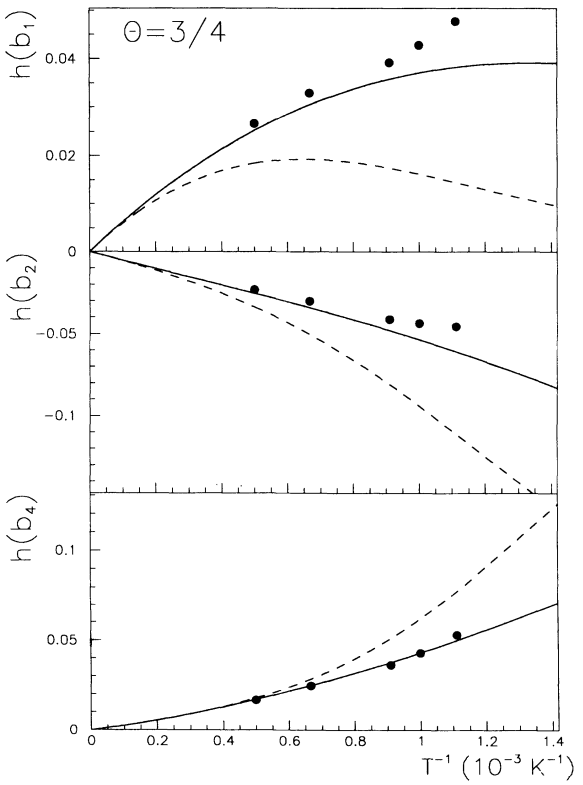

FIG. 10. The same as in Fig. 7, but at $\Theta = \frac{3}{4}$.

ence theory [25], which can be considered as a liquid-state version of the renormalization-group approach.

The PY2 and HNC2 equations should also give the three-point correlation function, which is important in the calculation of the diffusion coefficients. Usually the three-point correlation function is evaluated in the Kirkwood superposition approximation [10]. In a recent paper [26] it has been shown that the Kirkwood approximation is not accurate for the hard-sphere liquid; therefore, also in lattice gases more sophisticated approximations, such as PY2 and HNC2, might be necessary.

Finally, another topic of interest in the field of adsorbed layers is the study of the properties of systems with three-body interactions. By means of those interactions, which are of course important at high coverages, the asymmetry of the phase diagrams with respect to $\Theta=\frac{1}{2}$ can be explained [1]. Recently, three-body potentials have been introduced in the HNC closure for three-dimensional liquids [27]; the discretized version of this closure might be useful in the study of the properties of adsorbed layers at high coverages.

ACKNOWLEDGMENTS

This work has been partially supported by Consorzio Interuniversitario Nazionale per la Fisica della Materia, Unità di Genova, and by Centro di Fisica delle Superfici e delle Basse Temperature del Consiglio Nazionale delle Ricerche.

[1] B. N. J. Persson, Surf. Sci. Rep. **15**, 1 (1992).
[2] M. Schick, Prog. Surf. Sci. **11**, 245 (1981).
[3] D. P. Landau, in *Phase Transitions in Surface Films 2*, Vol. 267 of *NATO Advanced Study Institute, Series B: Physics*, edited by H. Taub, G. Torzo, H. J. Lauter, and S. C. Fain, Jr. (Plenum, New York, 1991), p. 11.
[4] G. Doyen, G. Ertl, and M. Plancher, J. Chem. Phys. **62**, 2957 (1975).
[5] R. J. Behm, K. Christmann, and G. Ertl, Surf. Sci. **99**, 320 (1980).
[6] K. Binder and D. P. Landau, Surf. Sci. **108**, 503 (1981).
[7] E. D. Williams, S. L. Cunningham, and W. H. Weinberg, J. Chem. Phys. **68**, 4688 (1978).
[8] M. Tringides and R. Gomer, Surf. Sci. **145**, 121 (1984).
[9] L. D. Roelofs and D. L. Kriebel, J. Phys. C **20**, 2937 (1987).
[10] J. P. Hansen and I. R. McDonald, *Theory of Simple Liquids* (Academic, London, 1976).
[11] R. Ferrando and E. Scalas, Surf. Sci. **281**, 178 (1993).
[12] R. Gomer, Rep. Prog. Phys. **53**, 917 (1990), and references therein.
[13] R. J. Baxter and I. G. Enting, J. Phys. A **11**, 2463 (1978).
[14] H. Cheng and T. T. Wu, Phys. Rev. **164**, 719 (1967).
[15] R. Brout, *Phase Transitions* (Benjamin, New York, 1965).
[16] N. H. March and M. P. Tosi, *Atomic Dynamics in Liquids* (Dover, New York, 1991).
[17] R. Balescu, *Equilibrium and Nonequilibrium Statistical Mechanics* (Wiley, New York, 1975).
[18] S. M. Foiles, N. W. Ashcroft, and L. Reatto, J. Chem. Phys. **80**, 4441 (1984).
[19] A. Parola and L. Reatto, Nuovo Cimento D **6**, 215 (1985).
[20] A. Parola and L. Reatto, Physica A **125**, 255 (1984).
[21] D. Levesque and L. Verlet, Phys. Lett. **11**, 36 (1964).
[22] L. Belloni, J. Chem. Phys. **98**, 8080 (1993).
[23] G. C. Wang, T. M. Lu, and M. G. Lagally, J. Chem. Phys. **69**, 479 (1978).
[24] R. Ferrando and E. Scalas, Surf. Sci. **287/288**, 907 (1993).
[25] A. Parola and L. Reatto, Phys. Rev. A **31**, 3309 (1985); A. Meroni, A. Parola, and L. Reatto, *ibid.* **42**, 6104 (1990).
[26] B. Bildstein and G. Kahl, Phys. Rev. E **47**, 1712 (1993).
[27] P. Attard, Phys. Rev. A **45**, 3659 (1992).